Design Analysis of a High Speed Copper Rotor Induction Motor for a Traction Application

Nicolas Rivière
MotorDesign Limited
Wrexham, UK
nicolas.riviere@motor-design.com

Giuseppe Volpe
MotorDesign Limited
Wrexham, UK
giuseppe.volpe@motor-design.com

Marco Villani
University of l'Aquila
L'Aquila, Italy
marco.villani@univaq.it

Giuseppe Fabri
University of l'Aquila
L'Aquila, Italy
giuseppe.fabri@univaq.it

Lino Di Leonardo
University of l'Aquila
L'Aquila, Italy
dileonardolino@gmail.com

Mircea Popescu
MotorDesign Limited
Wrexham, UK
mircea.popescu@motor-design.com

***Abstract*—This paper deals with the design of a 200kW, 20krpm machine for an electric vehicle application. The aim of the research is to design a low cost, rare-earth free magnet electric motor while ensuring mass production feasibility and providing higher performance than currently available technologies. Electromagnetic, thermal and mechanical constraints are considered throughout the machine design process, from the specification to the optimization. Rotor die-casting, oil spray cooling and hairpin winding are among the solutions investigated to fulfill the project requirements. Analytical and numerical methods are adopted for electromagnetic and continuous performance calculations over the machine's full speed range, taking into account the mechanical limits from a stress and modal point of view.**

Keywords—induction machine, high speed application, optimization, oil spray cooling, die-casting, hairpin winding

I. INTRODUCTION

The Electric Vehicles' (EVs) market has seen a significantly growth over the last decade, due to the new environmental restrictions provided by governments, in order to reduce gas emissions and to prepare the ecological transition towards the fossil fuel independency [1]. Compared to conventional combustion engines, the electric motors benefit of higher efficiency, braking recovery and they provide a noise free solution with a smoother driving, bettering passengers and pedestrians comfort. In order to limit the overall vehicle energy consumption and to ensure a modular integration, the market demand tends towards more efficient, lighter and more compact electric motors.

The present study focuses on the development of the next generation electric powertrains, avoiding the use of permanent magnets and ensuring the industrial feasibility for mass production with low manufacturing costs. The Induction Machine (IM) is therefore considered as a potential candidate. The main project specifications are reported in TABLE I. The Key Performance Indicators (KPIs), including efficiency, specific torque, specific power and power density are defined based on the Tesla 60S electrical machine [2]. Additional boundary conditions are set based on the vehicle requirements, considering the Jaguar XJMY21 as a target.

II. MACHINE TOPOLOGY

The IM topology with copper rotor cage is chosen to meet the project requirements. Even if the IM presents a lower efficiency and torque density than PM motors, the technology is well established and used in the automotive industry (e.g. Tesla Motors). It represents an attractive and feasible solution for EVs, due to simplicity, robustness and versatility reasons in addition to cost-effective manufacturing aspects and fault tolerant capability [3]. The copper is usually preferred to the aluminium owing to its higher electrical conductivity, higher mechanical strength and better thermal properties.

There are several solutions, not yet widely investigated when considering IMs as traction motors in EVs, including copper rotor die-casting, hairpin stator winding technology, high speed operation and oil spray cooling. Therefore, these solutions are here reviewed and addressed in the present study.

TABLE I. MOTOR SPECIFICATIONS

Parameter	Unit	Value	Comment
Specific power	kW/kg	≥ 4.3	Peak value, 30% increase based on Tesla 60S (active parts only)
Specific torque	Nm/kg	≥ 8.2	Peak value, 30% increase based on Tesla 60S (active parts only)
Power density	kW/l	≥ 8	Peak value, active volume only
Maximum speed	krpm	20	From Jaguar XJMY21 vehicle (230kph)
Peak power	kW	200	30s, up to base speed (≈ 5200rpm)
Peak torque	Nm	370	Up to base speed
Nominal torque	Nm	152	@ Low speed (≈ 2000rpm)
Nominal power	kW	70	@ Maximum speed
Efficiency	%	≥ 96	Peak value
		≥ 94.5	Over WLTP3 drive cycle
Phase current	A_{rms}	≤ 500	@720Vdc
Housing diameter	mm	≤ 250	-
Machine length	mm	≤ 310	Including housing and bearings
Active weight	kg	≤ 44.6	Based on KPIs and torque-power requirements

A. *High speed machines*

Being the output power obtained as the product of torque and speed, an increase of the machine operating frequency inherently increases its power density. This statement is true only if the airgap magnetic pressure (namely the product of the linear current density and the airgap magnetic flux density) is maintained to a certain level [4].

High speed machines present higher frequency dependent losses (i.e. iron, mechanical and AC copper losses), which are dependent on magnetic and current densities. Therefore, one of the biggest challenges, in the design process of high speed machines, is to keep these losses as low as possible and to extract them efficiently. This implies to make thoughtful electromagnetic and thermal choices.

From a mechanical point of view, the rotor may be subjected to high stresses and critical resonances that limit its dimensions [5]. In point of fact, for given materials and speed, a larger rotor will induce higher rotational stress due to centrifugal forces while a long and slim rotor will involve more hazardous bending modes.

B. *Die-casted vs fabricated rotor*

Four main types of rotor construction exist today for the IM: fabricated aluminium, fabricated copper, aluminium die-cast and copper die-cast. Nowadays, only the first three topologies have been commonly used. However, due to last decade technology improvements, the copper die-casting solutions are now industry proven and they present attractive features for high speed applications [6].

Compared to the fabricated copper case, the die-casted copper rotor IM suffers from lower efficiency [7]. In fact, during the die-casting process, the high temperature required to melt the copper (about 1093°C) can short-circuit the rotor core laminations, leading to additional eddy current losses. On the other hand, the die-casting itself gives a sturdiest rotor structure, which is more suitable for withstanding high centrifugal pressures at high speed.

Regarding the fabricated rotor manufacturing, additional attention must be paid to the end-ring assembly, where the brazing process may alter the electrical and mechanical connection between the parts in contact, resulting in lower electromagnetic performance and poorer mechanical resistance.

C. *Hairpin stator winding*

The investigated design makes use of the great performance of the proprietary hairpin stator winding. Each individual section has a characteristic hairpin like shape and it is formed of rectangular profile conductors, as shown in Fig. 1. This technology suits well for distributed windings and leads to repeatable manufacturing and robust construction at the critical connections between conductors [9].

Compared to traditional round wire winding, the hairpin one benefits of a higher slot fill factor (up to 0.75) and shorter end connections for a given number of poles, improving the machine performance and reducing its overall length. The thermal dissipation through the slots is also improved, since rectangular stator slots provide a snug fit for the conductors, hence a thermal path within the slots [9, 10].

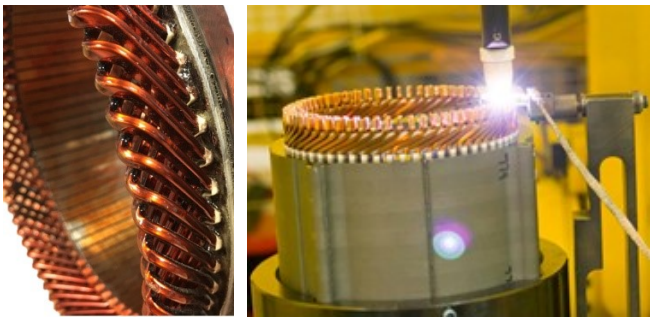

Fig. 1. Hairpin winding technology

The main drawback of this winding topology is the limited number of conductors that can pass through the slot, nowadays limited to 8. This leads to stator designs with big conductors, which can be problematic, especially in case of high speed applications. In this case, special attention to the AC winding losses component is required, due to significant high frequency skin and proximity effects [11].

D. *Oil spray cooling*

One of the investigated solutions to cool the machine makes use of oil spray. For instance, the oil can be thrown from nozzles placed on the shaft onto the inner winding ends' surfaces with a certain pressure. The coolant can also be dripped or sprayed over the outer surfaces from the housing or from the endcaps [12]. A sump then collects the fluid that is finally passed through a heat exchanger. This principle is illustrated in Fig. 2. This cooling configuration has the advantage of improving the heat transfer around the winding and rotor ends regions. In addition, the same fluid could be shared with the transmission apparatus.

III. MACHINE DESIGN

A complete design procedure is essential to validate the specifications before committing to make any physical prototype [13]. The logic behind the design process is outlined in Fig. 3. The first task consists in finding an initial design based on the main requirements such as torque, power, maximum speed and available space. During this stage, preliminary design choices are taken in order to properly chose fundamental parameters such as the slot/pole/bar combination, the optimal winding pattern, the main dimensions and the active materials. The obtained design can then be used as a starting point for the optimization.

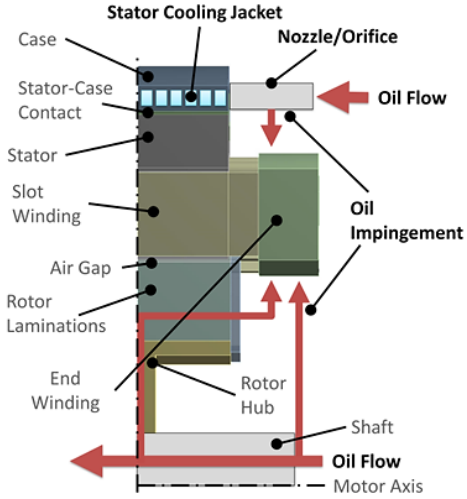

Fig. 2. Oil spray cooling principle [12]

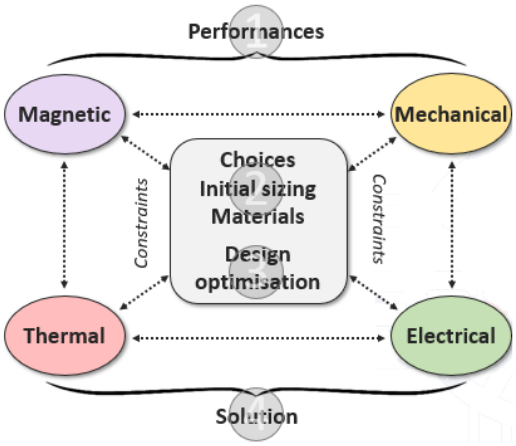

Fig. 3. Example of design procedure

A. *Electromagnetic design*

1) Geometry

The proposed initial design is shown in Fig. 4. Main parameters are summarized in TABLE II. The 4 pole, 36 slots, 50 bars topology appeared to be the most recommended combination for further optimization.

For mechanical reasons, the rotor slots are closed. Important to note that the design is already within the limits in terms of active weight and dimensions.

2) Winding

The winding layout is shown in Fig. 5. The main characteristics are given in TABLE III. A double layer pattern with four conductors per slot is selected to ensure the production feasibility.

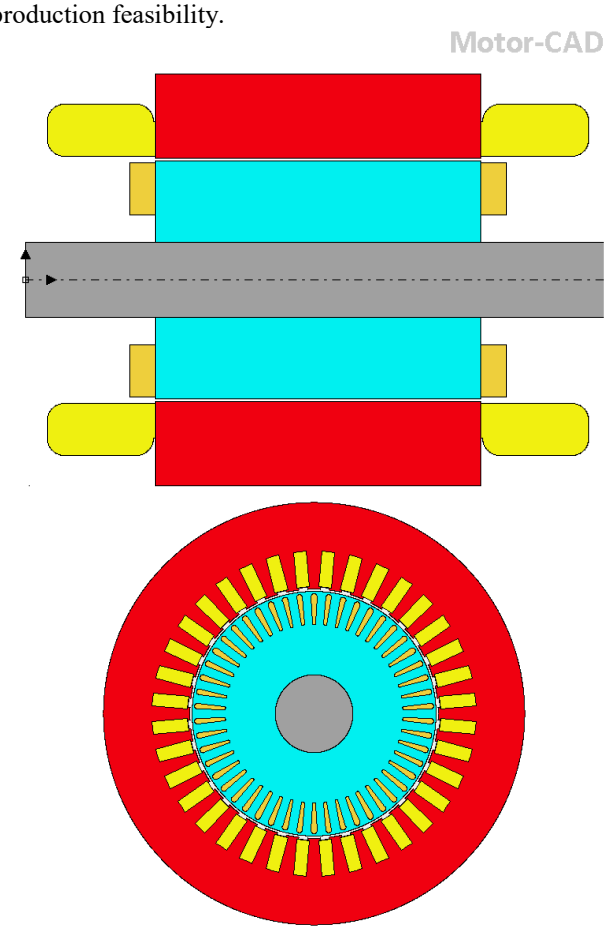

Fig. 4. Axial and radial machine geometry sections

TABLE II. MAIN STRUCTURAL PARAMETERS

Parameter	Unit	Value
Stator slots	-	36
Pole pairs	-	2
Rotor bars	-	50
Stator outer diameter	mm	190
Rotor outer diameter	mm	110
Airgap length	mm	1
Active length	mm	150
Active weight	kg	36

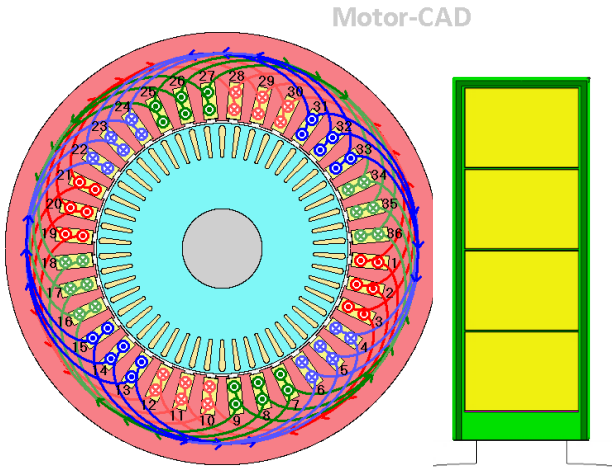

Fig. 5. Winding pattern and slot conductors

TABLE III. MAIN WINDING PARAMETERS

Parameter	Unit	Value
Conductors per slot	-	4
Turns per coil	-	2
Parallel path	-	1
Coil pitch	slots	9
Wire width	mm	5.60
Wire height	mm	3.35
Copper slot fill factor	%	73

The three phases are star-connected and they have coils in series to meet the inverter requirements.

The winding overhangs are 50mm long based on Tecnomatic expertise in the field, project partner in charge of the hairpin winding manufacture.

3) Materials

The selection of the materials for the IM rotor includes electrical steels and copper alloys.

In order to meet the KPIs along with the cost restrictions, materials with the best compromise between cost and performance have been selected.

The chosen materials must be already on the market and commercially available, in order to have detailed material properties and characterizations (magnetic, mechanical…) before simulations and manufacturing processes.

a) Electrical steels

Tests measurements on different non-oriented silicon-iron steel samples cut by laser were performed by RINA-CSM (project partner), for different frequencies (up to 1kHz) and different magnetic flux density (up to 1.6T) levels:

- M235-35A, fully process, 0.35mm thick,
- M290-50JKE, fully process, 0.35mm thick,
- NO30-15, fully process, 0.3mm thick,
- NO20-HS, fully process, 0.20mm thick.

For simplicity, only the characterizations at 400Hz are here presented (Fig. 6). The common M235-35A material was chosen considering the cost/performance compromise. Fig. 7 shows the relative permeability versus magnetic flux density for the selected material. The blue dotted line corresponds to the measured data while the red dotted line corresponds to the catalogue data. The difference is mainly due to the cutting effect.

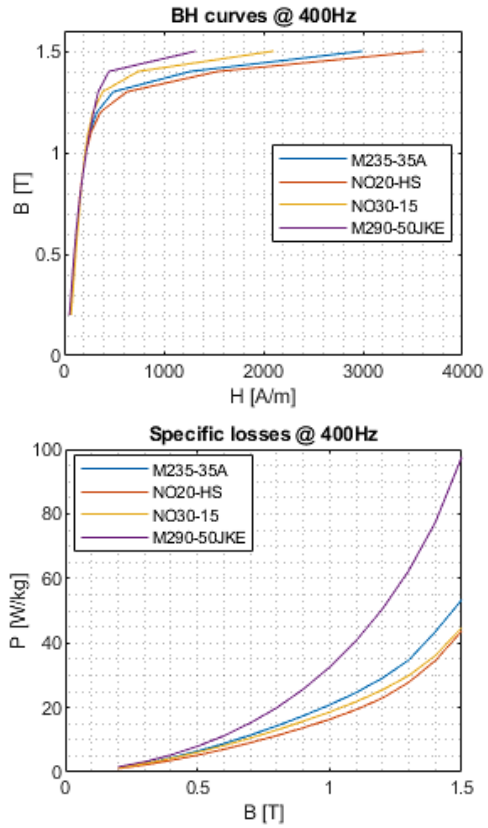

Fig. 6. Materials' characterizations at 400Hz

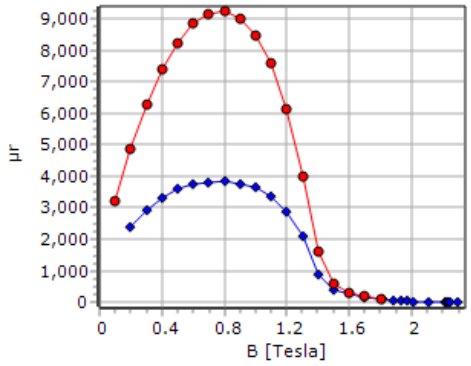

Fig. 7. Relative permeability data (M235-35A)

b) Copper alloys

Based on Aurubis and Breuckmann, project partners in charge of the fabricated and die-casted rotor manufacture, respectively, typical alloys are selected: CuAg0.04 (fabricated) and Cu-ETP (die-casted). In the first case, two filler materials are proposed depending on the assembly process: SAC-305 for soldered end-rings and Bercoweld-K5 for welded end-rings.

Electromagnetically, the difference between these solutions relies on the equivalent rotor resistance. TABLE IV shows similar values for the three resistances calculated with Motor-CAD software, leading therefore to similar performance. Must be said, that for the fabricated rotor resistance calculation, the filler material was assumed to occupy 10% of the end-rings' volume, value approved by Aurubis.

From a mechanical point of view, the selected alloys have enough strength to withstand the stresses induced in the rotor in harsh conditions (c.f. II.B.1). However, retaining caps are recommended to keep the end-rings in place at full speed, especially for the fabricated rotor that cannot handle high shear pressures due to the filler material. The welding process usually brings more strength to the end-rings assembly compared to the soldering one, but, on the other hand, it is more expensive.

For deepening the study, two fabricated rotors with either welded or soldered end-rings will be prototyped.

4) Performance

The peak performance over the full speed range of the machine are calculated using Motor-CAD with a Maximum Torque per Ampere (MTPA) control strategy and considering the electrical limits specified in the introduction.

The efficiency maps are given in Fig. 8 and Fig. 9. The peak performance requirements are fulfilled. Also note that the mechanical losses (airgap windage and bearing friction losses) are not considered in these calculations.

The WLTP3 drive cycle is considered to evaluate the machine energy consumption. The torque-speed demand on the motor side is defined based on the vehicle model implemented into Motor-CAD, using the Jaguar XJMY21 as a reference.

TABLE IV. EQUIVALENT ROTOR RESISTANCES AT 120°C

Copper cage type	Resistance @ 120°C [Ω]
Die-casted	0.01973
Fabricated + soldered end-rings	0.02050
Fabricated + welded end-rings	0.01902

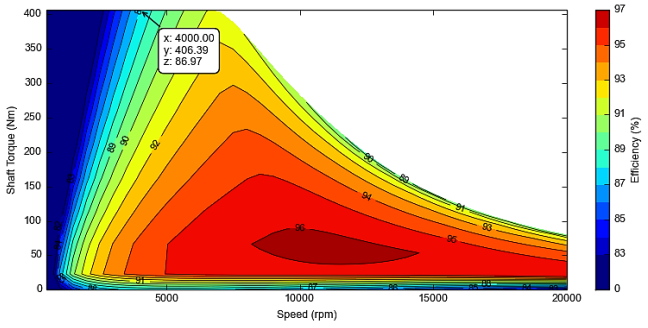

Fig. 8. Torque-speed efficiency map

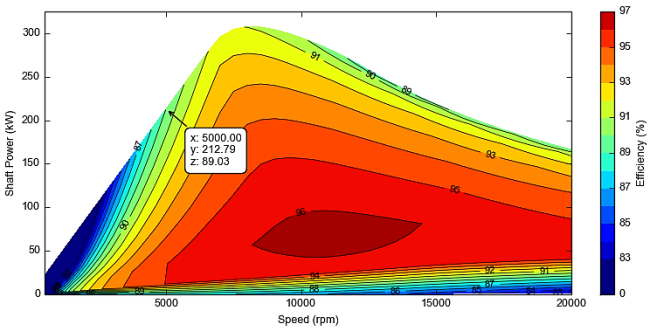

Fig. 9. Power-speed efficiency map

The efficiency calculated over the WLTP3 drive cycle for the proposed design is around 93.3%, which is less than the required value.

5) Conclusion

The main electromagnetic results are reported in TABLE V and compared with the target performances. All the requirements are met apart from the efficiency.

As a consequence, the optimization, that will be carried out at a later stage of the design, will focus on the loss reduction over the WLTP3 drive cycle.

B. Mechanical analysis

As mentioned before, high rotational speeds can lead to rotor mechanical failure in case of high stress or unstable resonance behaviour. Therefore, it is mandatory to design the rotor respecting the following criteria:

1. The operating frequency remains below the first natural frequency.
2. The maximum stress remains below the characteristic yield strengths of the materials.

Ideally, also the thermal stress due to the different expansion rates of materials in contact, or the stress induced by any clearance or interference fits, should be considered.

The properties, at room temperature, required for these analyses are reported in TABLE VI. The steel properties at 180°C are given in TABLE VII. The yield strength is assumed to drop down by 15-20% based on RINA-CSM experience. The Poisson's coefficient, density and thermal expansion coefficient are calculated by RINA-CSM using JMatPro software. All the other properties are assumed to be constant with temperature.

TABLE V. MAIN ELECTROMAGNETIC RESULTS

Parameter	Unit	Target	Calculated
Peak specific power	kW/kg	≥ 4.3	5.6
Peak specific torque	Nm/kg	≥ 8.2	10.2
Peak power density	kW/l	≥ 8	26.1
Peak power	kW	200	307
Peak torque	Nm	370	406
Peak efficiency	%	≥ 96	96
Efficiency over WLTP3		≥ 94.5	93.3
Phase current	A_{rms}	≤ 500	≤ 500
Machine length	mm	≤ 310	270
Active weight	kg	≤ 44.6	36

TABLE VI. ROTOR MECHANICAL PROPERTIES AT 22°C

Property	Unit	CuAg0.04	Cu-ETP	M235-35A
Density	kg/m^3	8940	8900	7530
Yield strength	MPa	320	150	423
Poisson's ratio	-	0.33	0.33	0.292
CTE[a]	10^{-5}/C	1.68	1.77	1.35
Young's modulus	GPa	107	100	190

[a.] Coefficient of Thermal Expansion

TABLE VII. STEEL MECHANICAL PROPERTIES AT 180°C

Property	Unit	M235-35A
Density	kg/m^3	7480
Yield strength	MPa	339
Poisson's ratio	-	0.298
CTE	10^{-5}/C	1.47

1) Stress analysis

A 2D FEA stress analysis is performed using ANSYS Mechanical software with a plane stress condition. Centrifugal forces and material expansions are considered for the analysis. The rotor bars are assumed to be perfectly bonded into the rotor slots. The model was reduced to one rotor slot pitch in order to decrease the computational time.

In Figs. 10 and 11, the Von-Mises stress distributions at 20% overspeed (24000rpm) are shown, for the two limit temperatures (22°C and 180°C). The maximum values are sufficiently below the materials' limits and the temperature effect is clearly visible in terms of stress migration towards the rotor slot bottom.

2) Modal analysis

A 3D FEA modal analysis is performed using ANSYS Mechanical software. Stiff bearings are considered, resulting in shaft modes only. The first natural frequency is 664Hz, which is sufficiently away from the maximum operating frequency (20000rpm/60 = 334Hz). For illustration, the two first bending modes of the rotor are shown in Fig. 12 and Fig. 13.

Fig. 10. Von-Mises stress @ 24000rpm, 22°C

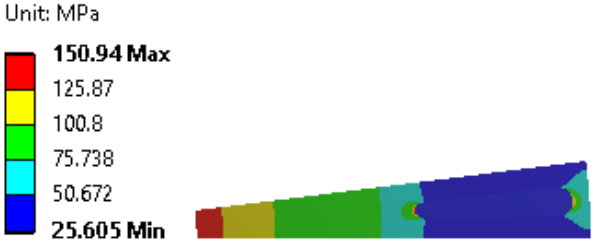

Fig. 11. Von-Mises stress @ 24000rpm, 180°C

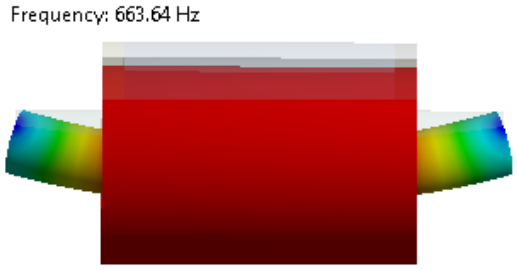

Fig. 12. First rotor bending mode

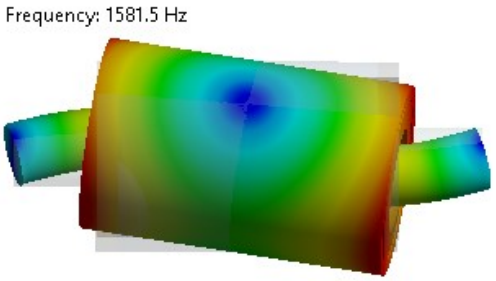

Fig. 13. Second rotor bending mode

C. Thermal design

From a thermal point of view, the machine is stator and rotor cooled. Two different solutions are investigated:

- ***Cooling #1***. It consists of a conventional housing Water Jacket (WJ) coupled with a shaft cooling system, using a mixture of ethylene, water and glycol as a coolant. A similar configuration can be found in the Tesla 60S and Audi E-tron motors [14].
- ***Cooling #2***. It is equipped with a spray cooling system with nozzles placed on the housing jacket and the hollow shaft surface, cooled by automatic transmission fluid.

1) Boundary conditions

Additional boundary conditions, specific to the cooling system design, are given in TABLE VIII. These include flow rate, pressure drop and temperature limits for the coolant and operating conditions.

Note that no value is mentioned for the pressure drop in the shaft cooling system, since it is affected by turbulences caused by the shaft rotation. Extensive CFD analyses would be required for such predictions. Alternatively, the channel dimensions and fluid velocity have been adjusted to acceptable values so as to limit the resulting pressure drop.

TABLE VIII. COOLING SYSTEM SPECIFICATIONS

Parameter	Unit	Value	Comment
Flow rate	l/min	≤ 10	Total flow rate share between the shaft and the housing
Pressure drop	kPa	≤ 20	Housing jacket only
Fluid outlet temperature	°C	≤ 90	Cooling #1 only
Ambient temperature	°C	50	-
Rotor cage temperature	°C	≤ 180	Limited by the bearings' thermal capability
Stator winding temperature	°C	≤ 180	Limit by the winding insulation class (H)

The axial views of the two cooling systems are reported in Fig. 14 and Fig. 15. They share the same package envelope with a diameter of 220mm and a length of 270mm.

2) Performance

The main characteristics of the cooling #1 and #2 are reported in TABLE IX. The continuous performance are shown in Fig. 16. Both configurations give plenty of power at high speed but run out of torque at low speed with respect to the specifications. As for the efficiency, the continuous torque in the low speed region needs to be optimized in order to meet the requirements.

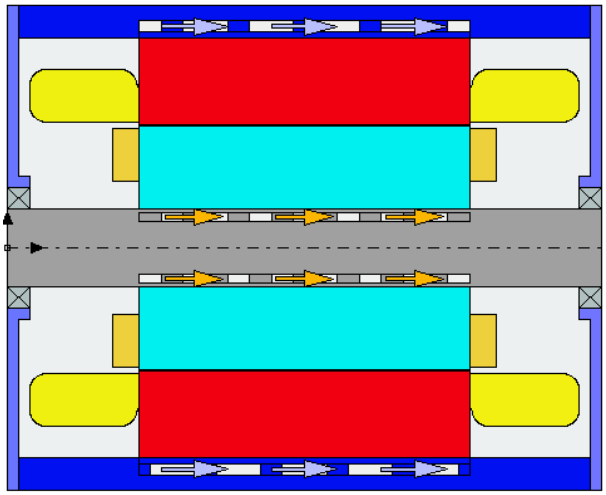

Fig. 14. Axial view of the Cooling #1

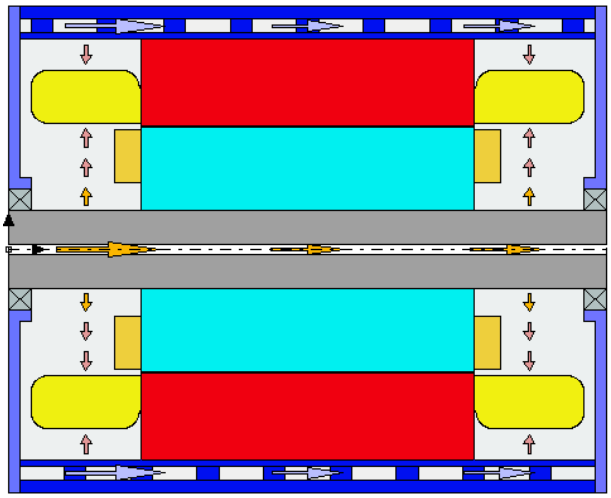

Fig. 15. Axial view of the Cooling #2

TABLE IX. MAIN THERMAL CHARACTERISTICS

Parameter	Unit	Housing		Shaft	
		#1	*#2*	*#1*	*#2*
Fluid inlet temperature	°C	65	90	65	90
Fluid outlet temperature	°C	75	98	80	107
Flow rate	l/min	8	4	2	2
Pressure drop	kPa	12.3	5.6	-	-
Diameter	mm	220		35	
Length	mm	270		270	

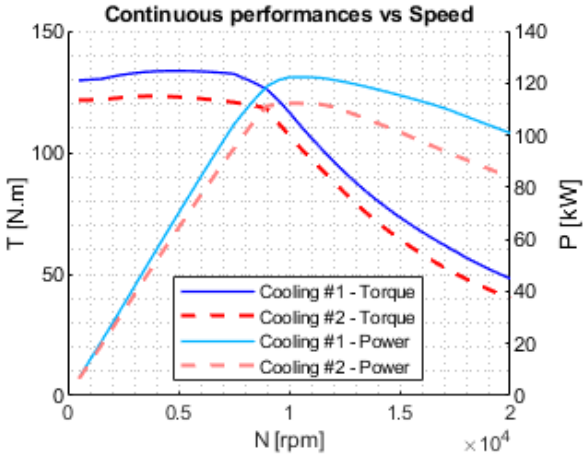

Fig. 16. Continuous performance

The maximum temperatures across the full speed range of the machine in the rotor cage and stator winding can give an insight of where to improve the heat dissipation (or where to minimize the losses). The rotor limits the thermal capability of the machine at low speed for both cooling types (Fig. 17).

Transient performance are also computed considering the base speed (5200rpm) and the maximum torque (370Nm) for 30 seconds. The results show that the machine is within its thermal limits (Fig. 18).

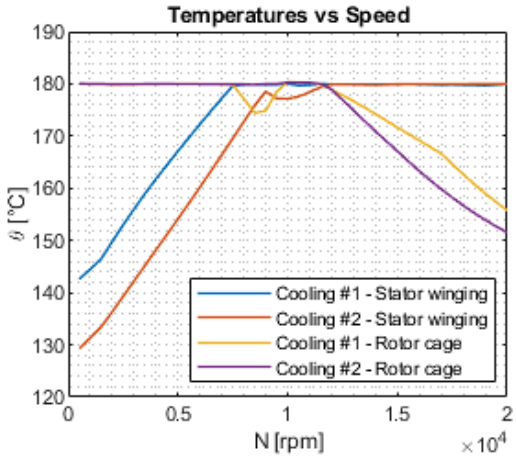

Fig. 17. Rotor cage and stator winding temperatures vs speed

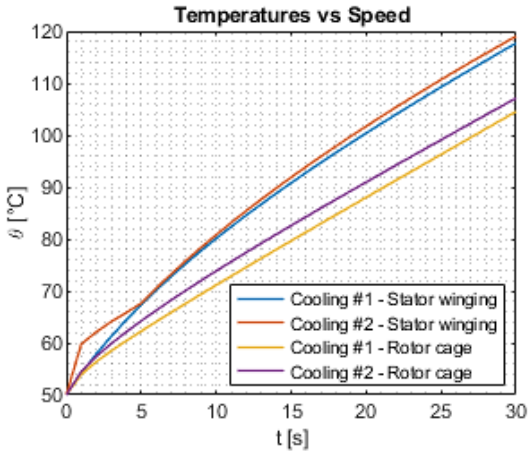

Fig. 18. Transient thermal performance

IV. Optimization Workflow

An optimization procedure has been set up using optiSLang software. Motor-CAD is driven from customized Python scripts in order to define, control and extract parameters of interest. A possible optimization workflow is presented in Fig. 19. First of all, a meta-model based sensitivity analysis is performed. The design space is scattered with different combinations of inputs. Then the optiSlang solver analyses the statistic variation and builds the best response surfaces, also called "Meta-models of Optimal Prognosis" (MOP), that represent the most important correlations between input parameters and responses. An optimizer can then be applied directly to the generated MOP. This strategy has the advantage to evaluate thousands of designs within minutes and it gives the designer an insight of where to concentrate the efforts for a given optimization problem. The following phase of the project will be focused on the optimization of the efficiency over the WLTP3 drive cycle together with the continuous performance at low speed.

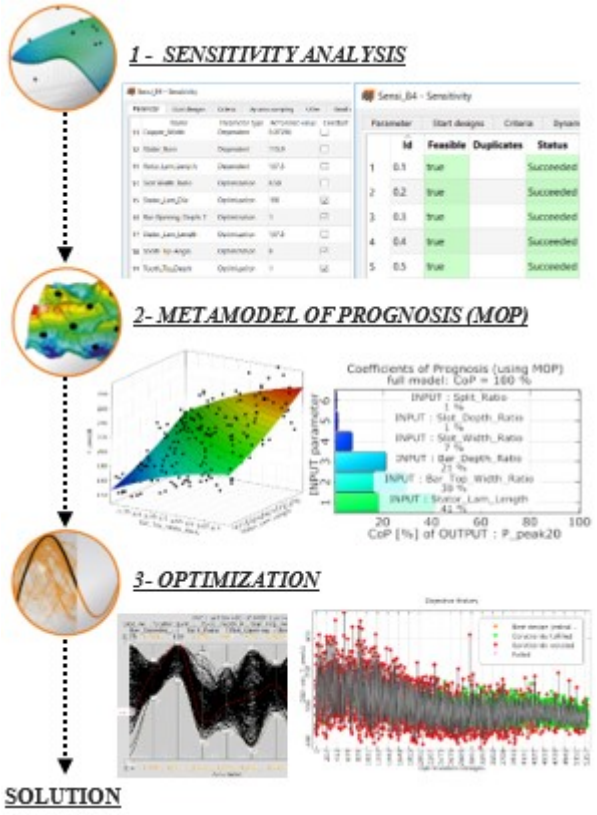

Fig. 19. Optimization workflow with optiSLang

V. Conclusion

This paper has presented the design analysis of a high speed copper rotor induction motor for an electrical vehicle application. The main project requirements are mass production feasibility, low cost and high performance.

New solutions for induction machines have been investigated, such as hairpin stator winding and oil spray cooling technologies. A proof of concept design has been proposed and it meets most of the given specifications.

The following steps, in the project, include the optimization of the efficiency over the WLTP3 drive cycle and of the machine's thermal capabilities.

ACKNOWLEDGMENT

This project has received funding from the European Union's Horizon 2020 Research and Innovation Programme under the Grant Agreement No 770143.

REFERENCES

[1] *Electric vehicles will grow from 3 million to 125 millions by 2030, International Energy Agency forecasts*, CNBC, 2018 [Online].

[2] *Tesla model S pricing and specs revealed*, MotorWard, 2011 [Online].

[3] M. Burwell, J. Goss and M. Popescu, "Performance/Cost comparison of the induction motor and permanent magnet motor in a hybrid electric car" TechnoFrontier 2013, Tokyo, Japan.

[4] J. Pyrhonen, T. Jokinen, V. Hrabovcova, *Design of Rotating Electrical Machines*. Chichester, UK,: Wiley, 2008.

[5] J. Huppunen, "High speed solid rotor induction machines – electromagnetic calculation and design", Ph.D dissertation, Dept. Elec. Eng., Lappeenranta Univ. Technol., Lappeenranta, Finland, 2004.

[6] R. Tiwari, Dr. A.K. Bhardwaj, "*Analysis of induction motor with die-cast rotor*". International Journal of Innovative Research in Electrical, Electronics, Instrumentation and Control Engineering, Vol 2, Issue 6.

[7] P. Carosa, W. Ripple, J. Kirtley, D. Seger, J. Sanner, M. Burwell, "Improving the Efficiency of High Speed Induction Motors Using Die Cast Copper Rotors", AC Propulsion, Report 2013.

[8] G. J. Grant, S. Jana, D. Catalini, B. Carlson, J. Agapiou, R. Szymanski, *"Novel Manufacturing Technologies for Hig Power Induction and Permanent Magnet Electric Motors",* 2015 DOE Vehicle Technologies Program, annual merit review and peer evaluation meeing, Washington, 2015.

[9] *Inside the HVH hybrid motor – Technical insights on Remy's "off-the-shelf" hybrid motor solutions*, White Paper, Remy Electric Motors, 2009.

[10] *Tecnomatic helps automakers design specialty assembly processes for advanced stator technologies,* Charged, Issue 37, 2018 [Online].

[11] P. Ponomarev, I. Petrov, N. Bianchi, J. Pyrhönen, "*Additional Losses in Stator Slot Windings of Permanent Magnet Synchronous Machines*", 10.13140/RG.2.1.2081.9368.

[12] K. Bennion, G. Moreno, "*Convective Heat Transfer Coefficients of Automatic Transmission Fluid Jets with implications for Electric Machine Thermal Management*", International Technical Conference and Exhibition on Packaging and Integration of Electronic and Photonic Microsystems, San Francisco, 2015.

[13] M. Rosu, P. Zhou, D. Lin, D. Ionel, M. Popescu, F. Blaabjerg, V. Rallabandi, D. Staton, "*Multiphysics Simulation by Design for Electrical Machines, Power Electronics, and Drives"*, IEEE Press, Wiley, New-York, 2018.

[14] *A detailed look under the Audi E-tron EV,* Carlist, 2018 [Online]